

Fig. 2. Longueurs (\AA) et angles ($^\circ$) de liaison. La numérotation des atomes est identique à celles de la Fig. 1.

Le Tableau 1 donne les coordonnées des atomes, le Tableau 2 donne les distances interatomiques et les angles de liaison.

Discussion. La Fig. 1 montre une vue en perspective de la molécule et la Fig. 2 montre les longueurs et les angles de liaison. La géométrie moléculaire est octaédrique. Si on compare les distances interatomiques de $\text{Cr}(\text{CO})_5\text{-}(\text{CS})$ à celles de $\text{Cr}(\text{CO})_6$ (Whitaker & Jeffery, 1967; Jost *et al.*, 1975), on remarque que la présence d'une fraction de CS sur chacun des six sites de coordination du chrome allonge significativement les distances Cr—O et C—O, conséquence d'une augmentation du rayon atomique de l'oxygène dans $\text{Cr}(\text{CO})_5\text{(CS)}$. Par contre le trop grand désordre statistique ne permet pas de déceler de raccourcissement de la liaison Cr—C dû à l'effet plus fortement liant du thiocarbonyle. La substitution préférentielle du soufre sur O(1), O(2) et O(3) plutôt que sur O(4) peut s'expliquer par l'environ-

Tableau 3. Distances intermoléculaires oxygène—oxygène (\AA) les plus courtes relativement à la molécule I (x, y, z)

O(1)…O(2) ^{II}	3,76	O(2)…O(4) ^{VIII}	3,48
O(1)…O(2) ^{III}	3,64	O(3)…O(3) ^{VIII}	3,70
O(1)…O(3) ^{III}	3,67	O(3)…O(3) ^{IX}	3,57
O(1)…O(4) ^{II}	3,57	O(3)…O(4) ^{IV}	3,46
O(1)…O(4) ^{IV}	3,62	O(3)…O(4) ^{VIII}	3,51
O(2)…O(3) ^V	3,53	O(3)…O(4) ^X	3,48
O(2)…O(3) ^V	3,62	O(4)…O(4) ^{IV}	3,62

Les chiffres romains sont relatifs aux molécules équivalentes suivantes:

(II)	$x, y, z + 1$	(VII)	$x - \frac{1}{2}, \bar{y} + \frac{1}{2}, \bar{z} - \frac{1}{2}$
(III)	$x + \frac{1}{2}, \bar{y} + \frac{1}{2}, \bar{z} + \frac{1}{2}$	(VIII)	$\bar{x}, \bar{y} + 1, \bar{z}$
(IV)	$\bar{x} + \frac{1}{2}, \bar{y} + 1, z + \frac{1}{2}$	(IX)	$x, \bar{y} + 1, \bar{z} + 1$
(V)	$x, y, z - 1$	(X)	$x - \frac{1}{2}, y, \bar{z} + \frac{1}{2}$
(VI)	$\bar{x}, y - \frac{1}{2}, \bar{z}$		

nement intermoléculaire, O(4) étant plus proche des atomes d'oxygène des molécules voisines que les autres atomes d'oxygène (Tableau 3).

Nous remercions J. Y. Thépot et G. Jaouen du Laboratoire de Chimie des Organométalliques de Rennes pour la préparation des échantillons et D. Bernard du Laboratoire de Chimie Minérale D, LA n° 254, Rennes, pour le test optique de centrosymétrie.

Références

- ENGLISH, A. M., PLOWMAN, K. R., BUTLER, I. S., JAOUEN, G., LE MAUX, P. & THÉPOT, A. (1977). *J. Organomet. Chem.* **132**, C1–C4.
 GERMAIN, G., MAIN, P. & WOOLFSON, M. M. (1971). *Acta Cryst. A* **27**, 368–376.
 JOST, A., REES, B. & YELON, W. B. (1975). *Acta Cryst. B* **31**, 2649–2658.
 SAILLARD, J. Y., LE BORGNE, G. & GRANDJEAN, D. (1975). *J. Organomet. Chem.* **94**, 409–416.
 WHITAKER, A. & JEFFERY, J. W. (1967). *Acta Cryst.* **23**, 977–989.

Structure of Cesium Neodymium Tetraphosphate

BY H. KOIZUMI AND J. NAKANO

Musashino Electrical Communication Laboratory, Nippon Telegraph and Telephone Public Corporation, Musashino-shi, Tokyo 180, Japan

(Received 15 March 1978; accepted 20 June 1978)

Abstract. $\text{CsNdP}_4\text{O}_{12}$, monoclinic, $P2_1$, $a = 7.123$ (2), $b = 9.152$ (3), $c = 8.782$ (2) \AA , $\beta = 99.72$ (3)°, $Z = 2$,

$U = 564.23 \text{ \AA}^3$, $D_x = 3.49 \text{ g cm}^{-3}$, $\mu(\text{Mo } K\alpha) = 141.6 \text{ cm}^{-1}$. The helical $(\text{PO}_3)_\infty$ chains, connected by isolated

NdO_8 dodecahedra and irregularly shaped Cs polyhedra, repeat after every eighth PO_4 tetrahedron along the b axis, in contrast to the helical chains in other alkaline Nd tetraphosphates with repeating units of four PO_4 groups. The refinement converged to $R = 0.038$ for 1334 independent reflections.

Introduction. Common features of the alkaline neodymium tetraphosphates $M\text{NdP}_4\text{O}_{12}$ (M^+ stands for Li, Na, K) previously reported are their helical chains of PO_4 tetrahedra linked by $-\text{Nd}^{3+}-M^+-$ chains along the shortest crystal axis, and the existence of mutually isolated NdO_8 dodecahedra (Hong, 1975a,b; Koizumi, 1976a,b). The only known exception in this series is $\text{RbNdP}_4\text{O}_{12}$, whose structure consists of the $[\text{P}_4\text{O}_{12}]^{4-}$ ring as in $(\text{NH}_4)\text{NdP}_4\text{O}_{12}$ (Koizumi & Nakano, 1977; Masse, Guitel & Durif, 1977).

Single crystals of $\text{CsNdP}_4\text{O}_{12}$ were grown from a $\text{CsPO}_3-\text{P}_2\text{O}_5$ melt by slow cooling. The starting melt was composed of 35 Cs_2O , 5 Nd_2O_3 and 60 P_2O_5 (mol%). The temperature of the melt was lowered at a constant rate of 1°C h^{-1} from 850°C down to 400°C . Thin platy or needle-shaped crystals, whose largest size was $2 \times 1 \times 0.3$ mm, were obtained.

Precession and Weissenberg photographs exhibited $2/m$ Laue symmetry with the unique systematic absence $0k0$ for $k = 2n + 1$. A prismatic crystal, whose dimensions were $0.18 \times 0.26 \times 0.40$ mm, was mounted so that its b axis was along the φ axis of the Rigaku Denki automatic four-circle X-ray diffractometer. Reflection data with $|F| > 3\sigma(F)$ up to $(\sin \theta)/\lambda = 0.65 \text{ \AA}^{-1}$ were measured with an $\omega-2\theta$ scan method using Mo $K\alpha$ radiation and a graphite monochromator. The intensities were corrected for Lorentz-polarization, absorption and extinction effects.

The intensity plot of Howells, Phillips & Rogers (1950) indicated a non-centrosymmetric structure;

therefore the space group $P2_1$ was assumed. From a three-dimensional Patterson synthesis, the probable locations of the heavy atoms, Nd and Cs, were found. These atomic coordinates gave an R value of 0.321 in the structure factor calculation. P and O positions were found by successive Fourier syntheses.

The structure was refined by the program ORFLS

Table 2. Bond distances (\AA) and angles ($^\circ$) in $\text{CsNdP}_4\text{O}_{12}$ with standard deviations in parentheses

Symmetry code

(i)	$1 - x, \frac{1}{2} + y, 1 - z$	(ii)	$1 + x, y, z$
(iii)	$x, y, 1 + z$	(iv)	$1 - x, \frac{1}{2} + y, -z$
(v)	$1 - x, y - \frac{1}{2}, 1 - z$	(vi)	$1 + x, y, 1 + z$
(vii)	$1 - x, y - \frac{1}{2}, -z$		

Dodecahedron around Nd

Nd—O(2 ⁱ)	2.40 (1)	Cs—O(2 ⁱ)	3.23 (1)
Nd—O(3 ⁱⁱ)	2.36 (2)	Cs—O(3 ⁱⁱ)	3.26 (2)
Nd—O(5)	2.55 (1)	Cs—O(5)	3.76 (1)
Nd—O(6 ^v)	2.33 (1)	Cs—O(6 ^v)	3.48 (1)
Nd—O(8)	2.33 (1)	Cs—O(7 ^v)	3.16 (1)
Nd—O(9)	2.50 (1)	Cs—O(8 ⁱⁱ)	3.94 (1)
Nd—O(11 ⁱⁱ)	2.49 (1)	Cs—O(9 ⁱⁱ)	3.16 (1)
Nd—O(12)	2.52 (1)	Cs—O(10 ^v)	3.48 (1)
Nd—Nd ⁱ	6.668 (7)	Cs—O(11 ^v)	3.63 (1)
Nd—Nd ^{iv}	6.792 (9)	Cs—O(11 ^v)	3.35 (1)
		Cs—O(12 ⁱ)	3.04 (1)

Tetrahedron around P(1)

P(1)—O(1)	1.60 (1)	O(1)—P(1)—O(2 ⁱⁱ)	110.9 (8)
P(1)—O(2 ⁱⁱ)	1.47 (1)	O(1)—P(1)—O(3 ^v)	106.5 (9)
P(1)—O(3 ^v)	1.49 (2)	O(1)—P(1)—O(4)	105.6 (8)
P(1)—O(4)	1.57 (2)	O(2 ⁱⁱ)—P(1)—O(3 ^v)	117.5 (9)
		O(2 ⁱⁱ)—P(1)—O(4)	109.9 (9)
		O(3 ^v)—P(1)—O(4)	105.7 (9)

Tetrahedron around P(2)

P(2)—O(4)	1.60 (2)	O(4)—P(2)—O(5)	116.0 (9)
P(2)—O(5)	1.45 (1)	O(4)—P(2)—O(6)	106.2 (9)
P(2)—O(6)	1.49 (1)	O(4)—P(2)—O(7)	96.8 (8)
P(2)—O(7)	1.62 (1)	O(5)—P(2)—O(6)	120.3 (8)
		O(5)—P(2)—O(7)	107.2 (9)
		O(6)—P(2)—O(7)	107.6 (8)

Tetrahedron around P(3)

P(3)—O(7)	1.55 (1)	O(7)—P(3)—O(8 ^{iv})	106.1 (8)
P(3)—O(8 ^{iv})	1.49 (1)	O(7)—P(3)—O(9)	108.0 (9)
P(3)—O(9)	1.48 (1)	O(7)—P(3)—O(10)	100.2 (8)
P(3)—O(10)	1.60 (1)	O(8 ^{iv})—P(3)—O(9)	121.8 (10)
		O(8 ^{iv})—P(3)—O(10)	105.0 (8)
		O(9)—P(3)—O(10)	113.1 (9)

Tetrahedron around P(4)

P(4)—O(10)	1.61 (1)	O(10)—P(4)—O(11)	106.0 (8)
P(4)—O(11)	1.50 (1)	O(10)—P(4)—O(12)	110.2 (8)
P(4)—O(12)	1.49 (1)	O(10)—P(4)—O(1 ⁱ)	100.0 (7)
P(4)—O(1 ⁱ)	1.59 (1)	O(11)—P(4)—O(12)	119.5 (9)
		O(11)—P(4)—O(1 ⁱ)	111.4 (9)
		O(12)—P(4)—O(1 ⁱ)	108.2 (8)

Inter-tetrahedral angle

P(1)—O(1)—P(4 ⁱ)	129.1 (7)
P(1)—O(4 ⁱ)—P(2)	144.5 (8)
P(2)—O(7)—P(3)	133.4 (7)
P(3)—O(10)—P(4)	131.6 (7)

Table 1. Final atomic coordinates

	x	y	z
Nd	0.7007 (0)	0.5016 (1)	0.3027 (0)
Cs	0.8283 (2)	0.6670 (2)	0.8251 (1)
P(1)	0.8559 (6)	0.1338 (5)	0.4585 (5)
P(2)	0.5596 (6)	0.8980 (5)	0.3770 (5)
P(3)	0.4181 (6)	0.7816 (5)	0.0705 (5)
P(4)	0.1921 (6)	0.5816 (5)	0.2269 (5)
O(1)	0.776 (2)	0.169 (2)	0.615 (1)
O(2)	0.043 (2)	0.062 (2)	0.493 (1)
O(3)	0.158 (2)	0.772 (2)	0.632 (2)
O(4)	0.707 (2)	0.028 (2)	0.365 (1)
O(5)	0.642 (2)	0.754 (1)	0.408 (1)
O(6)	0.420 (2)	0.956 (2)	0.471 (1)
O(7)	0.457 (2)	0.900 (1)	0.197 (1)
O(8)	0.643 (2)	0.361 (1)	0.078 (1)
O(9)	0.582 (2)	0.679 (2)	0.092 (1)
O(10)	0.228 (2)	0.710 (1)	0.110 (1)
O(11)	-0.012 (2)	0.537 (2)	0.180 (1)
O(12)	0.345 (2)	0.469 (1)	0.235 (1)

(Busing, Martin & Levy, 1962) with isotropic thermal factors, to give $R = 0.158$. Further cycles of least-squares refinement with anisotropic thermal factors reduced the R and R_w to 0.038 and 0.043, respectively. Final positional parameters are listed in Table 1.*

The atomic scattering and anomalous-dispersion factors for Nd^{3+} , Cs^+ , P and O listed in *International Tables for X-ray Crystallography* (1962) were used. The weighting scheme used during the final stages of the refinement was $w = (4.3 + |F_o| + 0.048|F_o|^2)^{-1}$.

Discussion. Bond distances and angles are given in Table 2. Views of the structure projected along the a and b axes are shown in Figs. 1 and 2. Fig. 3 represents the environments of the independent Nd, Cs and P atoms projected on (010).

The helical chains of the corner-shared PO_4 tetrahedra can be clearly seen on the (100) and (010) projections (Figs. 1, 2).

Although the $\text{CsNdP}_4\text{O}_{12}$ and $\text{KNdP}_4\text{O}_{12}$ crystals belong to the same space group, $P2_1$, the infinite screw $(\text{PO}_3)_\infty$ chains in the former are repeated after every eighth PO_4 tetrahedron along the b axis in contrast to the fourth PO_4 group along the a axis in the latter crystal (Hong, 1975a,b). Examples of similar periodicity in the screw $(\text{PO}_3)_\infty$ chain can be seen in the structures of $\text{CuK}_2(\text{PO}_3)_4$ and $\text{CoK}_2(\text{PO}_3)_4$ crystals (Tordjman & Guitel, 1974). The $\text{PbK}_2(\text{PO}_3)_4$ crystal also consists of $(\text{PO}_3)_\infty$ chains with eight PO_4 tetra-

* Lists of structure factors and anisotropic thermal parameters have been deposited with the British Library Lending Division as Supplementary Publication No. SUP 33709 (8 pp.). Copies may be obtained through The Executive Secretary, International Union of Crystallography, 5 Abbey Square, Chester CH1 2HU, England.

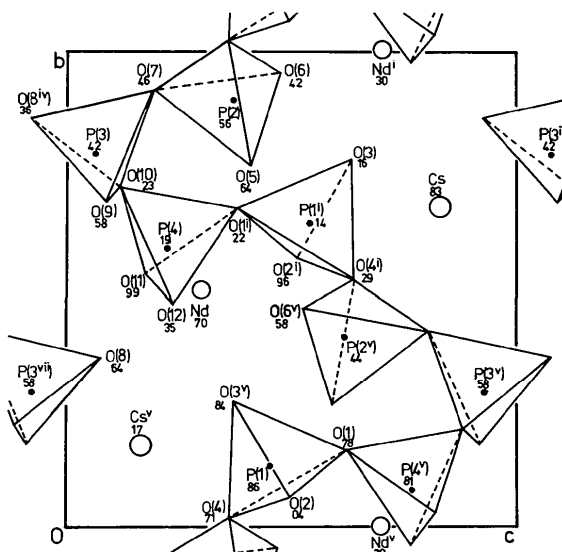


Fig. 1. The $\text{CsNdP}_4\text{O}_{12}$ structure projected along the a axis.

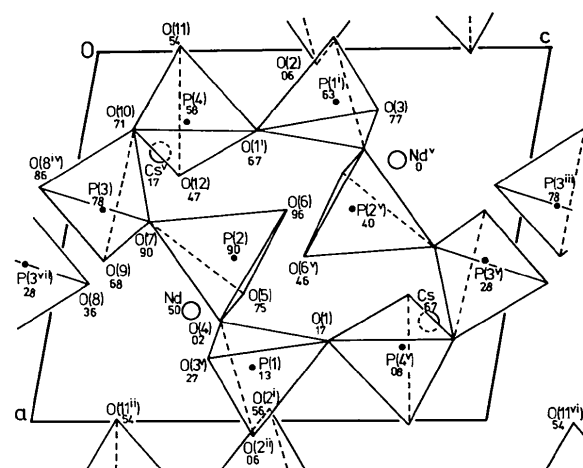


Fig. 2. The $\text{CsNdP}_4\text{O}_{12}$ structure projected along the b axis.

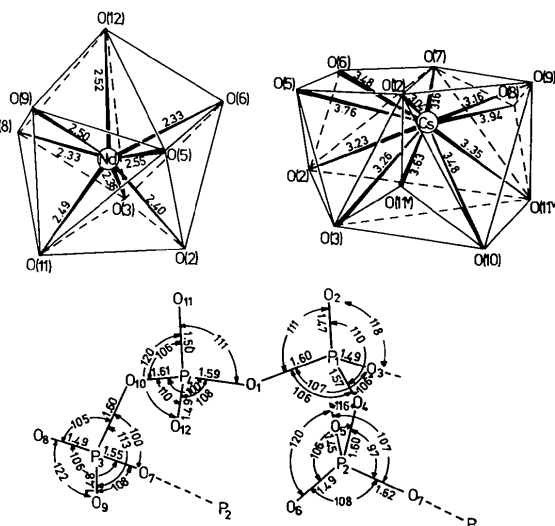


Fig. 3. Oxygen environments around the Nd, Cs and P atoms.

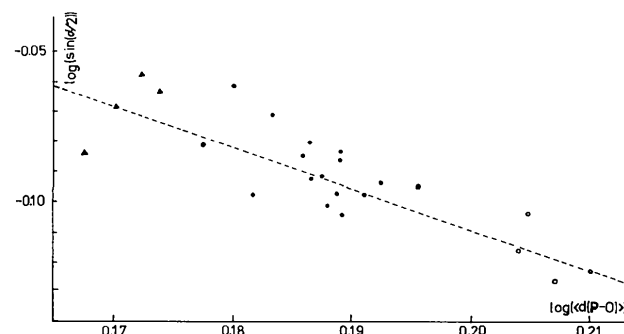


Fig. 4. Correlation between bond angles ($\angle \text{O}-\text{P}-\text{O}$) and their averaged bond lengths [$\langle d(\text{P}-\text{O}) \rangle$] in 24 independent $\text{O}-\text{P}-\text{O}$ groups. The symbols O, ● and ▲ illustrate the plots for the $\text{O}-\text{P}-\text{O}$ groups in which two, one and none, respectively, of their oxygen atoms take part in the bridging with adjacent PO_4 groups for the chain formation.

Table 3. *Electrostatic bond strengths in CsNdP₄O₁₂ (v.u.)*

	Cs ⁺	Nd ³⁺	P ⁵⁺ (1)	P ⁵⁺ (2)	P ⁵⁺ (3)	P ⁵⁺ (4)	\sum_o
O(1)	—	—	1.03	—	—	1.10	2.13
O(2)	0.12	0.41	1.45	—	—	—	1.90
O(3)	0.10	0.47	1.39	—	—	—	1.98
O(4)	—	—	1.13	1.05	—	—	2.18
O(5)	0.02	0.24	—	1.57	—	—	1.83
O(6)	0.05	0.51	—	1.40	—	—	1.95
O(7)	0.15	—	—	0.99	1.19	—	2.33
O(8)	0.01	0.51	—	—	1.37	—	1.89
O(9)	0.15	0.29	—	—	1.41	—	1.85
O(10)	0.05	—	—	—	1.04	1.05	2.14
O(11)	0.10	0.30	—	—	—	1.41	1.81
O(12)	0.26	0.27	—	—	—	1.44	1.97
\sum_c	1.01	3.00	5.00	5.01	5.01	5.00	

hedra in a repeating unit, but the structure is characterized by an 8/2 helix (8 units per 2 turns) along the chain axis, compared with the 8/1 helix with a large helical diameter in the present crystal (Brunel-Laügt & Guitel, 1977).

In order to estimate the distortion of the PO₄ tetrahedra in this structure, the following analysis was tried. Fig. 4 shows the correlation plots for the ratios of $\log[\langle d(P-O) \rangle]$ versus $\log[\sin(\alpha/2)]$ ($\alpha = \angle O-P-O$) in each of the 24 independent O-P-O angles listed in Table 2. These plots can be grouped into three regions as shown in Fig. 4, depending on how many O atoms in each O-P-O unit are taking part in the bridging with adjacent PO₄ groups for the chain formation. This curve nearly fits the correlation equation $\log[\sin(\alpha/2)] = 0.17 - 1.37 \log[\langle d(P-O) \rangle]$, which approximately agrees with the result of Baur's regression analysis for a condensed phosphate (Baur, 1970). It can be concluded that the contraction of P-O length with increasing π -bond nature in the O-P-O group causes an expansion of the O-P-O angle.

With respect to the transformation mechanism from cyclic tetraphosphate (RbNdP₄O₁₂) to linear tetraphosphate (CsNdP₄O₁₂), replacement of Rb⁺ by larger alkaline ions (Cs⁺) would cause a new combination between the P(1)O₄ group and the P(2)O₄ group [sharing O(4)] in place of the P(2')O₄ [sharing O(6')] (Fig. 2).

Although the NdO₈ dodecahedron is considerably distorted, no O atom is shared with the adjacent NdO₈. The NdO₈ group shares corners with the neighboring PO₄ tetrahedra, and faces [$\Delta O(2^i)$, O(5), O(6'); $\Delta O(8)$, O(9), O(11ⁱ)] and a corner [O(12)] with the neighboring Cs polyhedra. The shortest Nd-Nd distance (6.668 Å) has the largest value among the alkaline Nd tetraphosphate series.

Cs⁺ ions are surrounded by O atoms, except O(1) and O(4), with distances shorter than 4.00 Å. This type of irregularly shaped coordination around Cs⁺ can be seen also in the structures of Cs₂Mo₅O₁₆ and

Cs₂Mo₇O₂₂ (Gatehouse & Miskin, 1975) etc. (Fig. 3).

Bond strengths (S_i) for each cation coordination were calculated using the function $S_i = S_o(R_o/R_i)^{-N}$ proposed by Brown & Shannon (1973). The results are listed in Table 3. The bond-strength sums over the respective cation and O atoms seem to almost satisfy Pauling's electroneutrality relation (Pauling, 1948).

The authors are indebted to Dr N. Kamijo of the Government Industrial Research Institute, Osaka, for the intensity measurements. They also express their gratitude to Dr H. Iwasaki for his helpful discussion and encouragement.

References

- BAUR, W. H. (1970). *Trans. Am. Crystallogr. Assoc.* **6**, 129.
- BROWN, D. & SHANNON, R. D. (1973). *Acta Cryst.* **A29**, 266–282.
- BRUNEL-LAÜGT, M. & GUITEL, J. C. (1977). *Acta Cryst.* **B33**, 937–939.
- BUSING, W. R., MARTIN, K. O. & LEVY, H. A. (1962). ORFLS. Report ORNL-TM-305. Oak Ridge National Laboratory, Tennessee.
- GATEHOUSE, B. M. & MISKIN, B. K. (1975). *Acta Cryst.* **B31**, 1293–1299.
- HONG, H. Y.-P. (1975a). *Mater. Res. Bull.* **10**, 635–640.
- HONG, H. Y.-P. (1975b). *Mater. Res. Bull.* **10**, 1105–1110.
- HOWELLS, E. R., PHILLIPS, D. C. & ROGERS, D. (1950). *Acta Cryst.* **3**, 210–214.
- International Tables for X-ray Crystallography (1962). Vol. III, p. 258. Birmingham: Kynoch Press.
- KOIZUMI, H. (1976a). *Acta Cryst.* **B32**, 266–268.
- KOIZUMI, H. (1976b). *Acta Cryst.* **B32**, 2254–2256.
- KOIZUMI, H. & NAKANO, J. (1977). *Acta Cryst.* **B33**, 2680–2684.
- MASSE, R., GUITEL, J. C. & DURIF, A. (1977). *Acta Cryst.* **B33**, 630–632.
- PAULING, L. (1948). *J. Chem. Soc.* p. 1461.
- TORDJMAN, M. L. & GUITEL, J. C. (1974). *Acta Cryst.* **B30**, 1100–1104.